1 Introduction

Presently many types of spacecraft use a Spacecraft Attitude Control System (ACS) with momentum wheels for steering and electrochemical batteries to provide electrical power for the eclipse period of the spacecraft orbit. Future spacecraft will use Flywheels for combined use in ACS and Energy Storage. This can be done by using multiple wheels and varying the differential speed for ACS and varying the average speed for energy storage and recovery. Technology in these areas has improved since the 1990s so it is now feasible for flywheel systems to emerge from the laboratory for spacecraft use. This paper describes a new flywheel system that can be used for both ACS and energy storage.

Some of the possible advantages of a flywheel system are: lower total mass and volume, higher efficiency, less thermal impact, improved satellite integration schedule and complexity, simplified satellite orbital operations, longer life with lower risk, less pointing jitter, and greater capability for high-rate slews. In short, they have the potential to enable new types of missions and provide lower cost. Two basic types of flywheel configurations are the Flywheel Energy Storage System (FESS) and the Integrated Power and Attitude Control System (IPACS). The FESS is two identical and counter-rotating Flywheels with their rotating axis aligned. The IPACS is an orthogonal set of flywheels with spin axes in the x-y-z directions to perform three-momentum axis. An IPACS can also have two counter-rotating flywheels in each direction (total of 6 wheel) to provide zero, positive and negative momentum in each axis.

MagneMotion designed and constructed a flywheel energy storage system using a shaftless magnetic suspension. The suspension system is passively stable in all translational and rotational directions except for the axial direction, which is stabilized by control of current in coils integrated into the magnetic bearings. Careful attention to the shape of the composite rim allows a high energy density and by omitting the shaft it was possible to create a flywheel that has no critical resonances in the operating region. This design appears to have substantial advantage for either FESS or IPACS applications.

2 Flywheel system design

The MagneMotion flywheel system has no shaft and a permanent magnet suspension system with the following features:

- Feedback control to achieve stability at a point of lossless equilibrium in the axial direction;
- Passive radial guidance using the same magnets that provide axial suspension;
- Passive stability for the tilting axes;
- Composite rotor rim with a high energy storage density;
- No critical resonances in the normal operating region;
- Synchronous motor/alternator with a permanent magnet field inside the rotor rim;
- Minimal power loss in the speed range 10,000 to 60,000 RPM.

The flywheel was designed for a NASA application that required delivering 200 watts to a load for 30 minutes followed by a 60 minutes charge to return to the normal maximum

AAS 02-066

A Shaftless Magnetically Levitated Multifunctional Spacecraft Flywheel Storage System

Ken Stevens (MagneMotion Inc.)
Dr. Richard Thornton (MagneMotion Inc.)
Dr. Tracy Clark (MagneMotion Inc.)
Bob G. Beaman (GSFC, Electrical Systems Center)
Neil Dennehy (GSFC, GN&C Center)

25th ANNUAL AAS GUIDANCE AND CONTROL CONFERENCE

February 6-10, 2002
Breckenridge, Colorado

Sponsored by
Rocky Mountain Section

operating speed and with high round-trip energy efficiency. As the design evolved changes were made so the energy storage in the final design was less than 100 W-h. In a future design the wheel size can be changed so as to achieve almost any desired energy and momentum capability.

In order to achieve these objectives it was necessary to use a carefully balanced design that did not focus too much on any single parameter. For example: the design focused on achieving a high energy-to-mass ratio where the mass includes both the rotor and the stator, and it was necessary to use a rotor shape that is a compromise with many competing design issues. The intent was to create an integrated design that has high performance when evaluated as a complete system. Figure 1 is a simplified drawing that shows all of the key features. Figure 2 shows an exploded view of the flywheel with the rotor removed. The various components are discussed in the following sections.

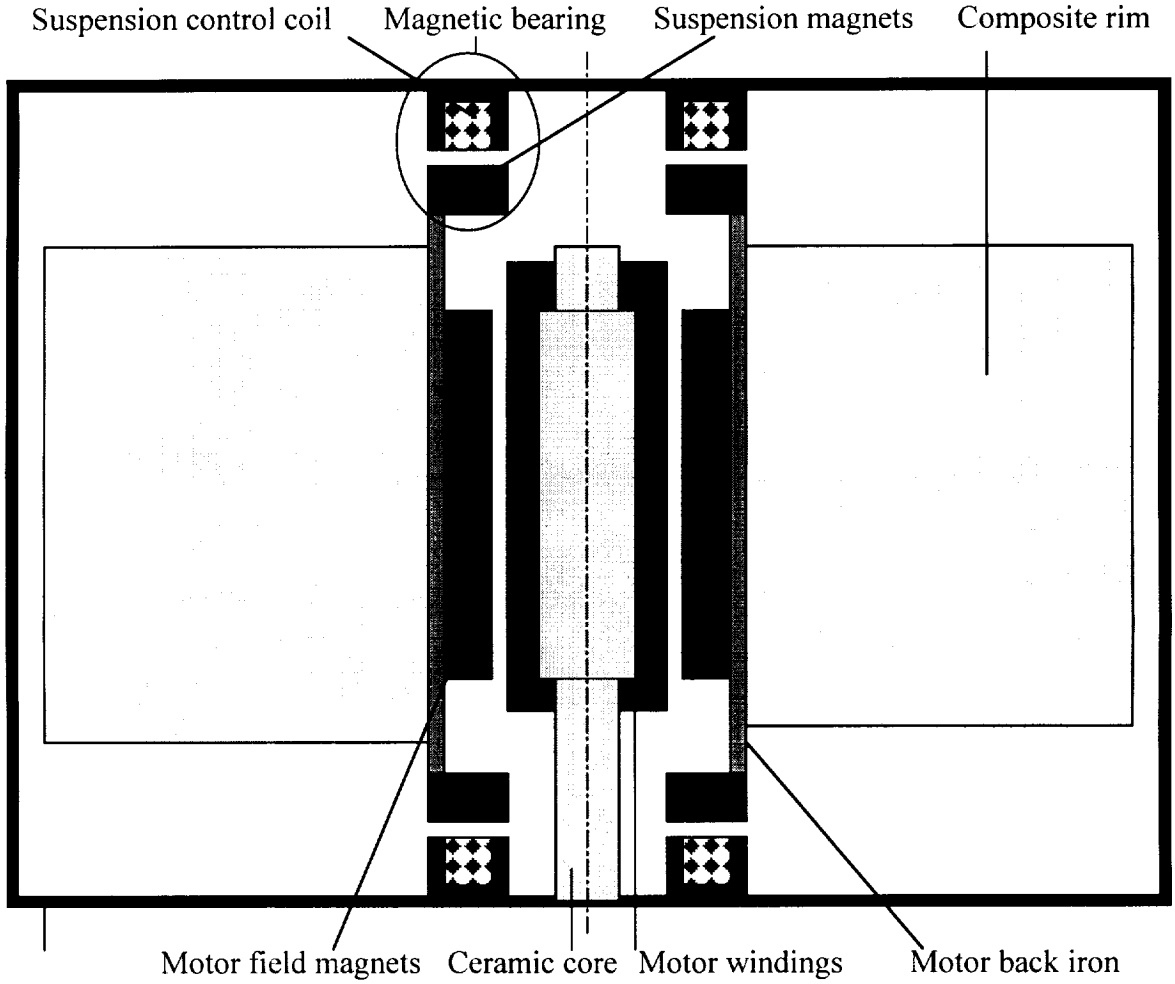

Fig. 1. Simplified cross section of flywheel energy storage system.

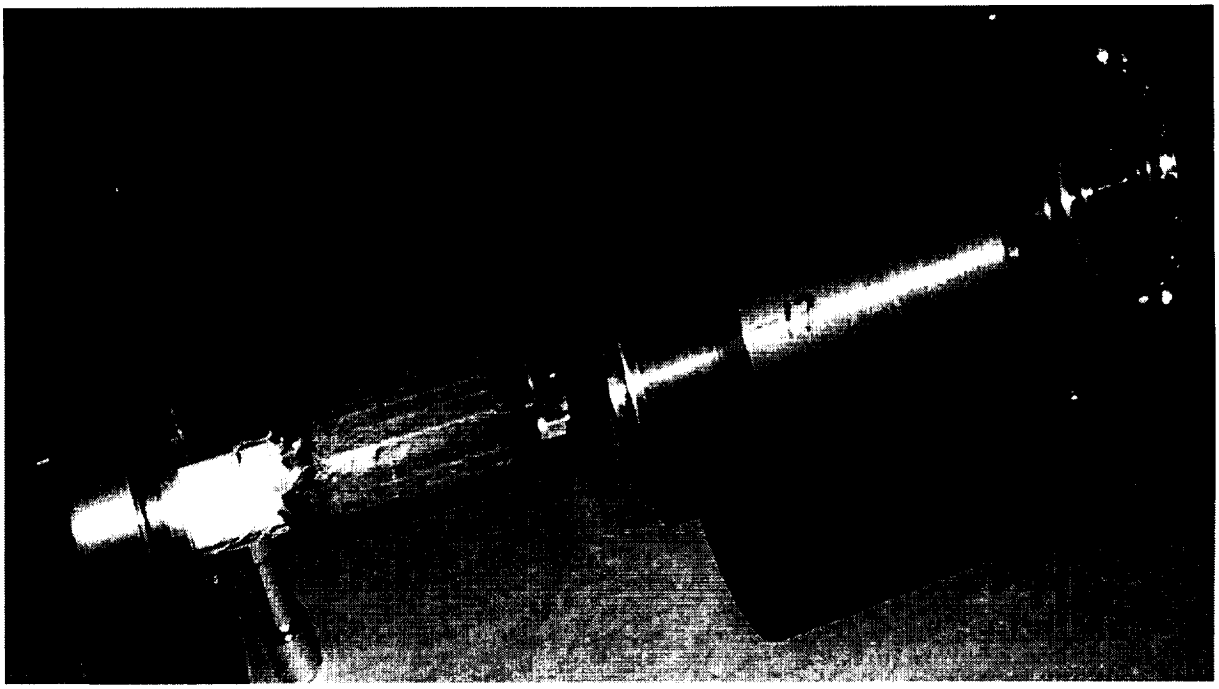

Fig. 2. Maglev flywheel system exploded view.

2.1 Magnetic suspension

There are magnetic bearings at each end of the rotational axis and each of these bearings creates a strong attractive force on the rotor. In gravity-free applications the rotor will have an equilibrium position with equal air gaps at each end. Control coils on the bearings are supplied from a control system that makes this a stable equilibrium position. For terrestrial applications the rotating axis is vertical and the top bearing will create sufficiently more force than the lower bearing to support the rotor mass. This will cause the air gap at the top to be somewhat smaller than the gap at the bottom. In Fig. 1 the upper bearing is labeled to show the various components of the magnetic suspension system. The magnets create a horizontal radial field that is focused by steel pole pieces to create an axial directed field across the air gap. This field provides both attractive and guidance forces. Ideally the permanent magnets provide all of the support so there is no power dissipation, but in operation a few watts of power will be consumed by the control system and in magnetic bearing losses.

If the rotor tends to move in a radial direction the bearings provide a restoring force that is proportional to displacement for all normal displacements. By making the spacing between bearings at least 2.5 times the diameter of the bearing the rotor is passively stable for tilting.

Note that at the higher speeds the rotor is rotating about its center of inertia so minor eccentricities in the bearing may not be a problem. However, bearing irregularities may create problems in power loss in the bearings.

2.2 Rotor

MagneMotion worked with Toray Composites (America) on the design of the rim. The wheel was then fabricated and spin tested to 45,000rpm by Toray. Final balancing to less that 0.09 gram inches was done by Lindskog Balancing, Boxborough, MA. The two most important issues in rotor design are to achieve the desired energy and momentum capability without exceeding the strength and fatigue limits of the materials, and to avoid large vibrations due to resonances at speeds of normal operation.

2.2.1 Rotor energy and momentum

The principal energy and momentum storage is in the composite rim part of the rotor. The rim was wound with carbon fiber that is very strong in the direction of the carbon filaments. The fiber was wound on a mandrel and pressed on to the rotor hub. This hub is also a mounting plate for the motor field magnets and provides a flux return path.

In the course of this project the composite rotor rim design went through several iterations but converged on the simple design, shown in Fig. 3. This shape provides a reasonable compromise between the many competing design factors and can be manufactured by a number of vendors. For weight-sensitive applications the rim can be constructed from carbon fiber and for cost-sensitive applications lower cost materials can be used with some degradation in energy density.

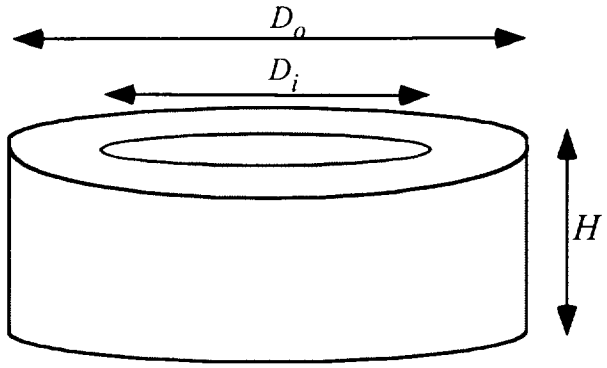

Fig. 3. Composite rim shape.

The composite rim has the following properties:

Mass: Rim (2.663)+Core(1.572 = 4.235 hg

Moment of Inertia: I=m*(di^2+do^2)/2 = .0115 kg-m^2

Kinetic Energy: Ke=I*(w^2-v^2)/2 watt-seconds, Or 121.3 Kwh

The prior discussion is for the composite rim only and did not include the effect of the inner core which provides less than 11% of the total energy storage but adds significantly to the rotor mass and moments of inertia. Table 1 gives the calculated values of parameters for the rim, the core and the complete rotor. The core properties are computed

on the basis of the mass density of steel and effective inner and outer diameters that give approximately the correct mass and moments of inertia. The composite rotor is 67% fiber and 33% resin and the component densities are: fiber 1,800, resin 1,150. The inertia ratio $\alpha = J_p/J_t$ is an important parameter in rotor dynamics and is discussed later.

Table 1. Rim and rotor parameters.

	Units	Rim	Core	Rotor
D_o	m	0.175	0.0625	0.175
D_i	m	0.0625	0.0465	0.045
H	m	0.08	0.15	0.15
ρ	kg/m^3	1586	7650	
m	kg	2.6626	1.5718	4.2343
J_p	kg-m^2	0.0115	0.0012	0.0127
J_t	kg-m^2	0.0072	0.0035	0.0107
α	-	1.6037	0.3365	1.1845

Table 2 gives the energy and momentum properties of the flywheel. For energy storage the intended speed range is 20,000 to 60,000 RPM so the net energy storage is 51.2 W-h. For ACS operation it may be desirable to work down to lower speed and the flywheel can provide operation over the range 10,000 to 60,000 RPM to achieve a net momentum capability of 66.1 J-s.

Table 2. Energy and momentum properties of flywheel at various speeds.

Speed	RPM	10,000	20,000	60,000
Energy	KJ	5.9	23.5	211.4
	W-h	1.6	6.5	58.7
Momentum	J-s	11.2	22.4	67.3

Figure 4 is a photograph of the rotor. The composite rim is primarily the shape shown in Fig. 3 but there is an extended inner portion that is attached to the steel core over its entire length.

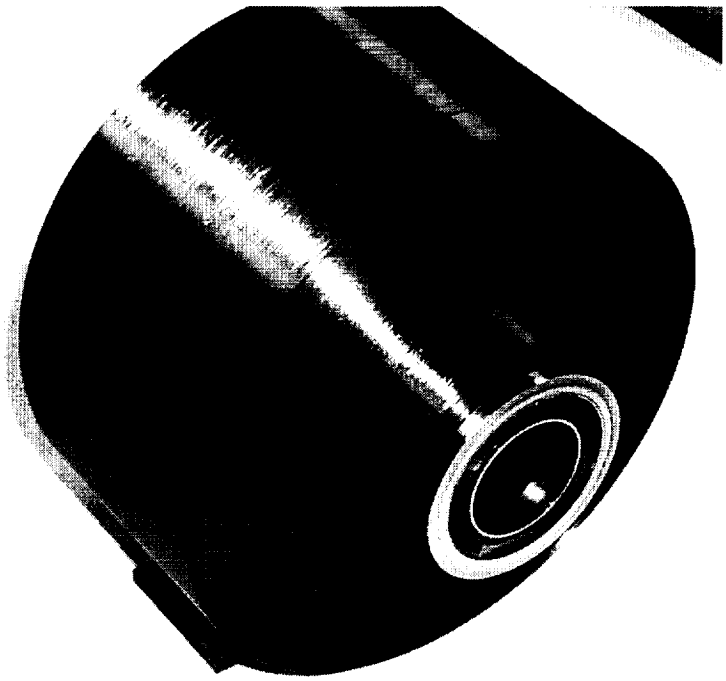

Fig. 4. Flywheel rotor.

The rim is built from several layers of winding in order to relieve stress and the resulting stress diagrams are shown in Figs. 4a and 4b. At 60,000 RPM there is adequate margin to prevent bursting even after millions of cycles of energy or momentum transfer.

Figures 5a and 5b show radial and hoop stress contour plots. Because the material can only carry moderate tensile radial stress it is desired to have this stress compressive. At 45,000 RPM the radial stresses at the composite rims interfaces are compressive. There is moderate tensile radial stress (<1.5 ksi) at the outer diameter of the outside composite rim. The transverse tensile strength of the material is in excess 3 ksi, resulting in positive margin. The hoop stresses in the composite rims varied from compression (-67 ksi) at the inner composite rim OD to 140 ksi tensile stress at the outer rim ID. Both the compressive and tensile hoop stresses are well within the material allowable (-3σ) strength capability shown in Table 3.

Table 3. Rim material properties (based on -3σ).

Property	T800H/RF007
Tensile (ksi)	490
Elongation (%)	1.21
Fiber direction Comp. (ksi)	138
Transverse tension (ksi)	>3 ksi
Transverse compression	65

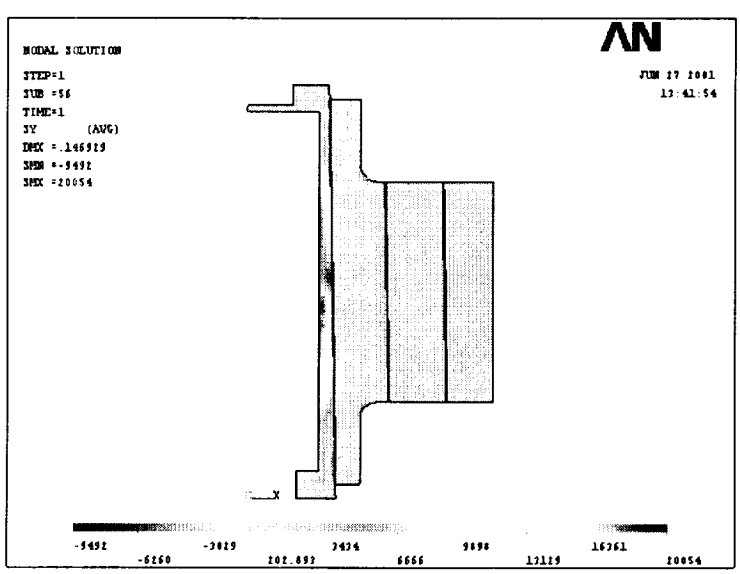

Figs. 5a. Radial stress in rotor.

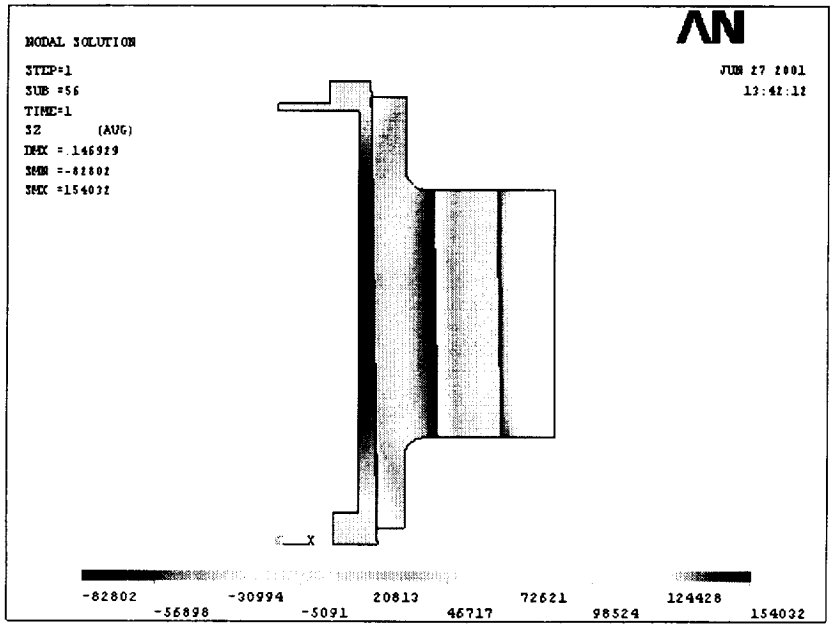

Figs. 5b. Hoop stress in rotor.

2.2.2 Rotor dynamics

The bearing and shaft interact to create a number of critical resonances and some of these can be in or below the normal operating region. It is common to operate rotating machinery above one or more of these resonances, but it is imperative not to operate too long at speeds near these values. For a flywheel system it is not possible to change the speed rapidly so it is desirable to eliminate critical resonances from the operating region. The elimination of the shaft can achieve this result but there are critical inertia ratios that must be maintained in order to avoid severe vibration problems.

For a rotating structure the critical resonances are typically highly underdamped (i.e. high Q) and sometimes even negatively damped, in which case the oscillations will grow until limited by the some other mechanism. The resonant frequencies are often functions of the rotational speed and can be further related to the direction of rotation. A good way to understand potential problems is to plot a "Campbell Diagram," such as the ones shown Figs. 6a and 6b for two different shaftless flywheel designs. In these Figures the dashed lines are plots of the rotational frequency against itself and the solid lines are plots of various resonant frequencies of the flywheel vs. the rotational frequency. If any of the solid lines cross the dashed line there can be severe oscillations at the frequency of intersection. Because of the high Q nature of the resonance, even a very small imbalance in the rotor is all it takes to produce unacceptably large vibrations at these rotational frequencies. Even if the dashed line is near the solid lines there can be severe vibration problems so the design problem is to avoid close proximity of the solid lines to the dashed line in the entire region of operation.

Figure 6a is a Campbell Diagram for a design with $\alpha = 0.96$, a flywheel with unacceptable behavior because the upper solid line tracks the dashed line up to high speeds. Figure 6b is a Campbell Diagram for the MagneMotion flywheel with $\alpha = 1.18$ and there is enough margin to minimize problems of vibrations due to rotor imbalance. The difference between these two figures is due to an assumed rim heights of 0.15 for unacceptable behavior and 0.08 for the final design that led to acceptable behavior. If the rim height is less than 0.08 the inertia ratio will increase because the properties of the core tend to dominate and this shows that flywheel dimensions are very critical and it is important to reduce the transverse moment of inertia of the core.

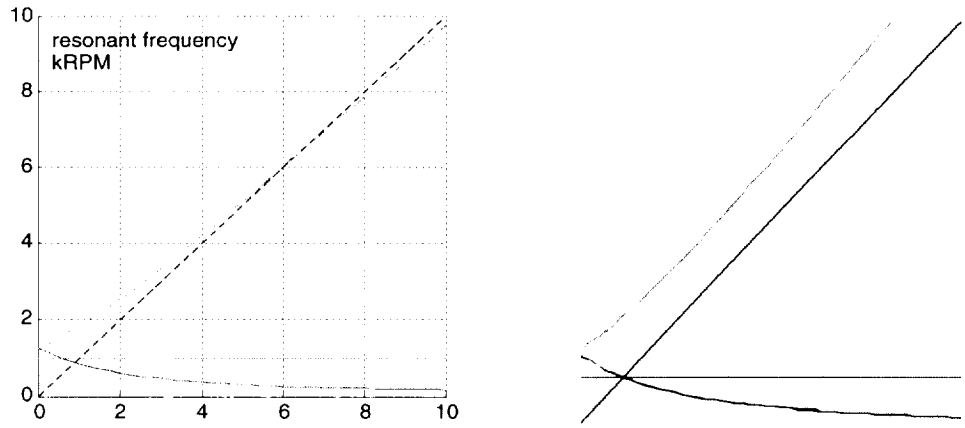

Figs. 6a and 6b. Campbell Diagrams for shaftless flywheels. The bearings are identical but the rim height is different leading to $\alpha = 0.96$ and $\alpha = 1.18$, the final design.

For all flywheels there is a low frequency resonance, approximately 1,000 RPM for the diagrams in Fig. 6. Well below this speed the rotor rotates about the center of force of the bearing while well above this speed the rotor rotates about the center of inertia of the

rotor. Near this speed there can be high amplitude vibrations due to even minor asymmetries in the rotor, but the flywheel is rotating so slowly that a touchdown bearing can be used to limit the amplitude of oscillation.

All flywheels will have other resonances, but flywheels with shafts will typically have a shaft-based resonance in the preferred operating region while shaftless flywheels can be designed to have no other resonances below the burst speed of the rotor. It was seen that moment of inertia ratio is a very important parameter that affects rotor dynamics. For a flywheel with the shape shown in Fig. 3 the ratio of the polar inertia, the inertia about the axis of rotation, to the transverse inertia is designated α and given by

$$\alpha = \frac{J_p}{J_t} = \frac{2}{1 + \frac{4H^2}{3\left(D_o^2 + D_i^2\right)}}$$

In order for the upper curve in Fig. 6 to not cross the dashed line we must have $\alpha > 1$.

This ratio can never be greater than 2.0 and to achieve $\alpha > 1$ requires: $D_o^2 + D_i^2 > \frac{4}{3}H^2$.

If D_i is small this becomes $D_o > 1.15\ H$. For adequate stability it is necessary to achieve $\alpha > 1.15$ and when the core properties are considered the rim should have $\alpha > 1.5$. In short, the rim should have $D_o > 2\ H$. The MagneMotion design meets this criteria and achieves $\alpha = 1.18$ leading to the Campbell Diagram shown in Fig. 6b. If the wheel is well balanced there should not be excessive vibration from 2,500 RPM to the bursting speed.

2.3 Motor/generator

The energy transfer to and from the flywheel is accomplished by a synchronous machine that serves as both a motor for accelerating the wheel and a generator for delivering useful power to a load. The motor uses a 6-pole, 3-phase design with the field provided by NdFeB magnets that produce a radially directed field in the region of the stator windings. The steel core of the flywheel serves as the path for the return flux from the magnets. There is no steel in the winding area.

Fig. 7 shows a photograph of the magnet array. It consists of 6 magnets, each spanning 85% of 1/6 of the circumference. Ideally the magnets would be magnetized radially, but this would have required a special magnetizing fixture and the modest performance improvement was not necessary for this prototype, so they were magnetized on a planar axis. It would have been possible to use a 4-pole array, but this would require thicker back iron and magnets and reduce the diameter of the winding. For larger flywheels, particularly when higher power output is required, it might be preferable to use a design with a modified Halbach Array for the magnet structure.

Fig. 7. Photograph of the inside of the rotor showing the magnet array.

Figure 2 shows the 3-phase winding wound on a ceramic core that serves as a rigid spacer for the winding and also conducts heat from the winding to the outer housing. Steel in the stator winding structure is avoided in order to eliminate destabilizing magnetic forces and to minimize losses due to eddy currents and hysteresis. This winding uses many strands of fine wire in order to minimize power loss associated with eddy currents in the wire. A rotary position sensor is located in the rotor and used to control the switching of currents in the winding. The controller can transfer energy to and from a DC power bus that is connected to a suitable energy source and also provides power to the load.

3 Test results

3.1 Magnetic suspension

The magnetic bearing was able to support the flywheel at the point of near-zero power dissipation in a gravity environment both in a normal atmosphere and inside of an evacuated chamber. The control system could maintain the magnetic gap during operation and there were no unexpected instabilities

3.2 Rotor

One of the wheels was burst tested at Test Devices in Hudson, MA. The burst speed was 79,500 RPM, 32% higher than the design speed of 60,000 RPM.

3.3 Motor/generator

The motor and generator functions worked well and there does not appear to be any need for major modifications. It was possible to transfer energy either way at a rate of well

over 200 watts over the entire design operating speed range. If required, the peak power can be increased by modifying the magnet array and using a longer rotor winding.

3.4 Operation

The prototype flywheel system was successfully operated at speeds up to 36 kRPM. The operational results obtained thus far are quite encouraging. The rotor is levitated from its parked position at zero speed and then accelerated to store energy in the wheel. The levitation system is stable at all speeds. The low-frequency bearing resonances at 1200 RPM and 2300 RPM are easily traversed as the wheel is accelerated up to its operating speed range. The motor/generator readily supplies the rated torque to the rotor over the tested speed range, allowing energy transfer into or out of the wheel.

The primary departure from expected operation lies in the measured drag associated with the spinning rotor. The simplest method to measure the drag is to spin the wheel up and then shut down the motor/generator to allow the wheel to coast down. The rate at which the wheel slows down is equal to the drag torque divided by the wheel inertia, so it is easy to plot the drag as a function of wheel speed as shown in Fig. 8. The data in Fig. 8 was taken with a speed measuring system that had low resolution so the small wiggles should be ignored. However, the big jumps near 1,200 and 2,300 RPM are due to vibrations near the frequency where the rotor shifts from rotating about the center of inertia of the wheel to the center of force of the bearing. In this region the touchdown bearing plays a crucial role and it would be inappropriate to operate in this speed range for long periods of time.

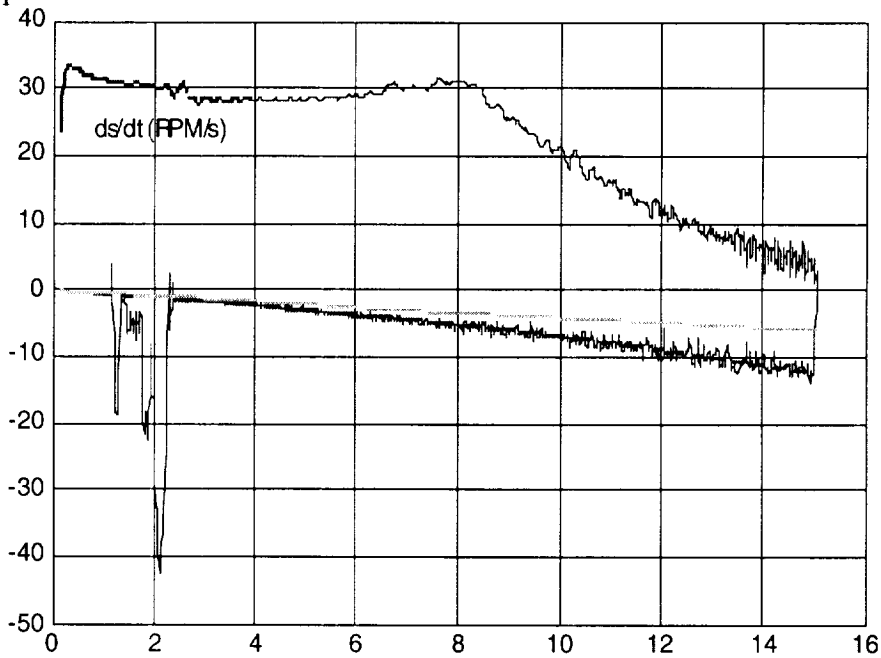

Figure 8. Speed-up and coast-down test.

Note that there are two drag terms, one that varies linearly with speed and one that varies as the square of speed. The square-law term is likely due to aerodynamic drag resulting

from a non-ideal vacuum. The rotor was tested at a vacuum of 15 Torr then at 0.5 Torr. The effect of the square law drag term was noted. The linear drag term is consistent with the model for the eddy-current losses associated with the stator windings in the motor/generator and steel poles in the levitation bearings.

The most important unanswered question is: Can the bearing losses be reduced to acceptable levels. Answering this question will be a key part of the next phase of development. Reducing loss will require careful attention to details, such as the quality of the vacuum, the precision of manufacture of the bearing and the uniformity of the magnetic field in the bearing. It is believed that the flywheel losses can be reduced to levels that make the flywheel a suitable part of a combined ACS and energy storage system.

4 System Applications

MagneMotion wheel parameters

EPS Flywheel Calculator, BGB 011221

Name of Flywheel			
Rotor Dimensions			
OD	0.1750 meters	ro	0.0875 meters
ID	0.0625 meters	ri	0.0313 meters
Height	0.08 meters	v	62832
Weight	2.6626 kg	w	376991
volume	0.00168 m^3		
Density	1586.0 kg/m^3		
Rotor Speed		Rotor Inerta	0.0115 kg m^2
Low Speed	10,000 RPM	Rotor Ke	794,010,098 watt seconds
Hi Speed	60,000 RPM		
		Energy Avalible	220.6 Kwh
System Mass		MAX SED	82.8 Kwh/kg
Mag Bearings	1.000 kg		
Motor Generator	0.500 kg		
Core	1.572 kg		
Mag Bearing controller	0.250 kg		
M/G Controller	0.250 kg		
Enclosure	0.250 kg		
Rotor	2.663 kg	Notes:	
TOTAL	6.484 kg	Graphite Den = 1.89 * 10^3 Kg/m^3	

Several types of spacecraft are looked at with this wheel application. The two wheel Momentum bias system and 3 axis stabilized systems are shown. This wheel size is not a cure all for every system, however the wheel can be scaled to fit the individual application.

	IMDC Proposed Spacecraft			
	Exist FF	GPM-3CS	GTWS-D	GEC-2
Battery System	100ah NiH2-IPV	35ah NiH2-IPV	110ah LiIon	23ah NiH2-CPV
Number of batteries	1	1	3	1
Capacity Required Whr	935	299	2,483	147
Weight kg	81.5	39.4	80	22
Energy density Whr/kg	11.47	7.59	31.04	6.70
Reaction Wheel System	Momentum biasis	3 axis Stabalized	3 axis Stabalized	Momentum biasis
Number of wheels	2	4	4	2
Torque, each wheel N-m			0.12	
Momentum N-m-s		11	11	
Max speed rpm				
Weight, system kg	24	29.2	29.2	35.46
Battery + Reaction Wheel Weight kg	105.5	68.6	109.2	57.46
Flywheels (120wh) required for an equivalent system	8	4	20	2
Flywheel weight kg	52	26	130	13
Weight savings by using flywheels kg	53.5	42.6	-20.8	44.46

BGB,020111

The GTWS-D spacecraft with LiIon batteries is expected to have a life of 2 years. For a longer life mission NiH2 battery would have to be used. This which would bring the Flywheel mass savings close to the EOS examples below.

	Existing Spacecraft				
	GOES	POES	EOS-PM1	Hubble	EOS-AM1
Battery System	12 ah NiCd	40 ah NiCd	160ah NiH2-IPV	90ah NiH2-IPV	50 ah HiH2-IPV
Number of batteries	2	3	1	6	2
Capacity Required Whr	460	575	1,405	1,700	1,976
Weight kg	20	113	200	422	284
Energy density Whr/kg	23.00	5.09	7.03	4.03	6.96
Reaction Wheel System					
Number of wheels	1&2	4	4	4	4
Torque, each wheel N-m	0.09,0.036	0.11	0.3	0.81	0.3
Momentum N-m-s	68,2.7	27	81	264	81
Max speed rpm	66,003,000	6400	6000	3700	6000
Weight, system kg	19.5	27.5	32	420	61.6
Battery + Reaction Wheel	39.5	140.5	232	842	345.6
Flywheels (120wh) required	4	4 (1)	12	14	18
Flywheel weight kg	26	26	78	91	117
Weight savings by using	13.5	114.5	154	751	228.6

BGB,020111

(1) For the POES spacecraft 150 wh was used instead of 120 wh.

5 Summary

It is believed that for many spacecraft applications the MagneMotion flywheel energy storage system can have a higher performance than current electrochemical battery energy storage systems. The controllable momentum of the flywheel then becomes available to perform a spacecraft steering function.